Molecular Therapy
Nucleic Acids
Original Article

CRISPR/Cas9-Mediated Three Nucleotide Insertion Corrects a Deletion Mutation in MRP1/ABCC1 and Restores Its Proper Folding and Function

Qinqin Xu,[1] Yue-xian Hou,[1] and Xiu-bao Chang[1]

[1]Department of Biochemistry & Molecular Biology, College of Medicine, Mayo Clinic in Arizona, Scottsdale, AZ 85259, USA

A three-nucleotide deletion in cystic fibrosis transmembrane conductance regulator/ATP-binding cassette transporter C7 (CFTR/ABCC7) resulting in the absence of phenylalanine at 508 leads to mis-fold of the mutated protein and causes cystic fibrosis. We have used a comparable three-nucleotide deletion mutant in another ABCC family member, multidrug resistance-associated protein (MRP1)/ABCC1, to determine whether CRISPR-Cas9-mediated recombination can safely and efficiently knock in three-nucleotide to correct the mutation. We have found that the rate of homology-directed recombination mediated by guideRNA (gRNA) complementary to the deletion mutant is significantly higher than the one mediated by gRNA complementary to the wild-type (WT) donor. In addition, the rate of homology-directed recombination mediated by gRNA complementary to the WT donor is significantly higher than that of gRNAs complementary to the 5′ or 3′ side of the deletion mutant. Interestingly, the frequency of mutations introduced by gRNA complementary to the deletion mutant is significantly higher than with gRNA complementary to WT donor. However, combination of gRNAs complementary to both WT donor and deletion mutant decreased the rate of homology-directed recombination, but did not significantly decrease the mutation rate introduced by this system. Thus, the data presented here provide guidance for designing of gRNA and donor DNA to do genome editing, especially to correct the mutations with three mismatched nucleotides, such as three-nucleotide deletion or insertion.

INTRODUCTION

Many genetic disorders, such as color blindness,[1–4] cystic fibrosis,[5,6] hemochromatosis,[7,8] hemophilia,[9–15] phenylketonuria,[16,17] polycystic kidney disease,[18,19] and sickle cell disease (https://ghr.nlm.nih.gov/condition/sickle-cell-disease), are caused by simple point mutations. For example, a deletion of three-nucleotide (nt) coding for phenylalanine at position of 508 (ΔF508) in the cystic fibrosis transmembrane conductance regulator (CFTR) or ATP-binding cassette transporter C7 (ABCC7) gene, the most common mutation in cystic fibrosis, results in thermolability and mis-folding of the CFTR/ABCC7 ion channel protein within the epithelial cells[20,21] and causes cystic fibrosis. Such disease-causing mutations can potentially be corrected by homology-directed recombination (HDR).

However, HDR is a complex processing of orchestrated reactions involving multiple factors. In addition, presynaptic single-strand DNA invasion (searching for homologous sequences) plays a crucial role for initiation of the HDR. The greatest challenge in HDR-mediated gene correction is the creation of recombinogenic DNA ends near the mutation site. Development of the CRISPR/Cas9 system provides a mean to cut the DNA (making either a nick or double-strand DNA break [DSB]) near the mutation site.[22–29] Unfortunately, non-homologous end-joining (NHEJ), albeit without ensuring restoration of the DNA sequence around the break site, plays a dominant role over HDR for any DSB repair in mammalian cells,[30–32] meaning that the efficiency of the HDR-mediated repair of the mutation near the CRISPR/Cas9-guideRNA (gRNA) cutting site could be very low. In addition, the modifications at the break site, including a few nucleotides insertion[33] and/or deletion,[34] may cause deleterious mutations, suggesting that safety is another very important issue in CRISPR/Cas9-mediated gene correction. Thus, evaluation of the relative contribution of NHEJ and HDR specifically to the repair of the CRISPR/Cas9-gRNA-mediated single-strand nick or DSB is critical in the design of strategies to correct mutations in genetic disease.

To evaluate the relative contribution of NHEJ and HDR specifically to the repair of the CRISPR/Cas9-mediated single-strand nick or DSB, we have used another ABCC family member, the multidrug resistance-associated protein (MRP1/ABCC1), as a model system in which we had shown previously that a single phenylalanine deletion (ΔF728) at a comparable position in nucleotide binding domain 1 (NBD1) as F508 in CFTR/ABCC7[35] causes similar mis-folding and loss of drug transport function. Cells expressing wild-type (WT) and ΔF728 MRP1/ABCC1 as well as monoclonal antibody (mAb) reagents developed during our earlier investigations of MRP1/ABCC1 greatly facilitate monitoring the optimization of gRNAs and other conditions for gene editing. In this model system, the expression of WT MRP1/ABCC1 mainly forms mature protein with an apparent

Received 23 February 2017; accepted 5 May 2017;
http://dx.doi.org/10.1016/j.omtn.2017.05.005.

Correspondence: Xiu-bao Chang, Department of Biochemistry & Molecular Biology, College of Medicine, Mayo Clinic in Arizona, 13400 East Shea Boulevard, Scottsdale, AZ 85259, USA.
E-mail: xbchang@mayo.edu

This is an open access article under the CC BY-NC-ND license (http://creativecommons.org/licenses/by-nc-nd/4.0/).

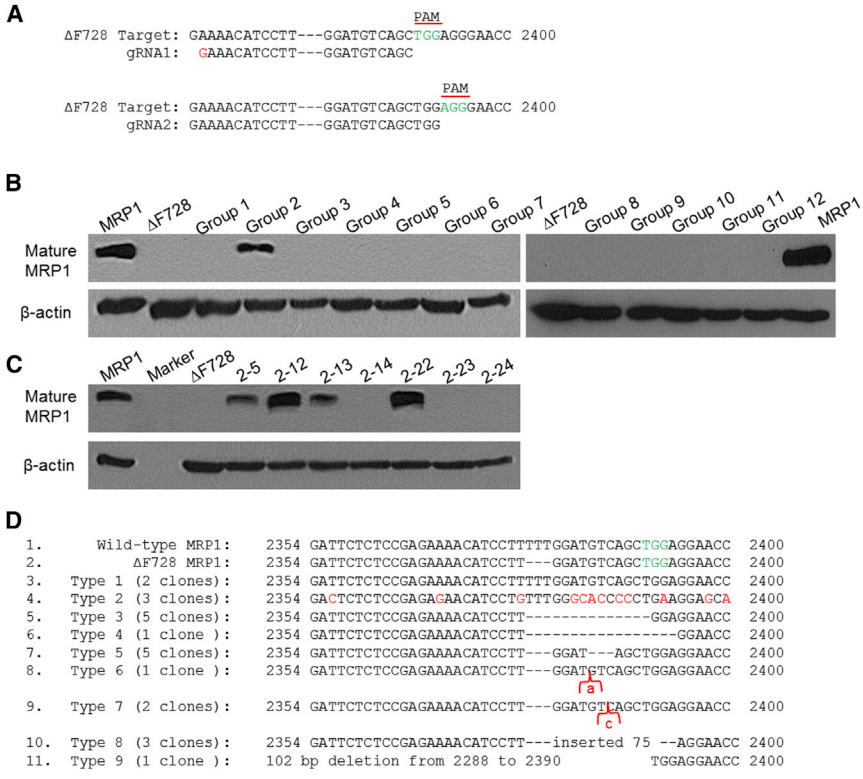

Figure 1. Effects of gRNAs Complementary to MRP1/ABCC1-ΔF728 Deletion Mutant on Knock In of the Three Deleted Nucleotides

(A) Design of gRNAs complementary to MRP1/ABCC1-ΔF728 deletion mutant. The red G indicates an artificially introduced G residue at the beginning of the gRNA1. The minus sign (–) indicates the deleted nucleotide. The green TGG or AGG indicate the PAM sequence for gRNA1 or gRNA2. (B) A representative western blot, probed with MRP1/ABCC1 mAb 42.4, showing the WT MRP1/ABCC1 protein generated by HDR. The WT MRP1 cell lysates, used as a positive control, were appropriately diluted with BHK cell lysates so that this band will not be over-developed. (C) A representative western blot, probed with MRP1/ABCC1 mAb 42.4, showing the WT MRP1/ABCC1 protein generated by HDR in isolated individual colonies from transfection group 2. (D) DNA sequence analyses of the clones derived from the reverse transcription products of total RNA isolated from 2-12. The number of clones in parentheses indicates the number of clones having the sequence. The red capital letters indicate the sequences that are not complementary to human MRP1/ABCC1. The small red letters indicate the inserted nucleotides.

molecular weight (MW) of ~190 kDa, which can be efficiently detected with our mAbs 42.4 and 897.2.[36] In contrast, the expression of MRP1/ABCC1-ΔF728 mainly forms an immature protein with an apparent MW of ~170 kDa that can be efficiently detected with 897.2, but not by 42.4, because F728 is part of our 42.4 mAb's epitope.[36] Thus, if MRP1/ABCC1-ΔF728 mutation is corrected, a mature band at ~190 kDa can be efficiently detected with our 42.4 mAb.

We have found that the rate of HDR mediated by gRNA complementary to ΔF728 mutated DNA is significantly higher than the one mediated by gRNA complementary to the WT donor DNA, whereas the rate of gene correction mediated by gRNA complementary to the WT donor DNA is significantly higher than those gRNAs complementary to either the 5′ side or 3′ side of MRP1/ABCC1-ΔF728. However, the mutation rate introduced by gRNA complementary to ΔF728 mutated DNA is significantly higher than the one mediated by gRNA complementary to the WT donor DNA. Thus, the data presented here provide a gRNA designing guidance for genome editing.

RESULTS

MRP1/ABCC1-ΔF728 Is Used as a Model System for Genome Editing

Deletion of phenylalanine 508 in CFTR/ABCC7, which is present in most cystic fibrosis patients, results in mis-processing of the ion channel protein within epithelial cells.[20,21] Deletion of the counterpart phenylalanine at position 728 in MRP1/ABCC1 also results in a similar thermolability and mis-folding of the drug transporter so that only the endoplasmic reticulum (ER)-retained immature form of the protein (~170 kDa) is detected by our MRP1/ABCC1 mAb 897.2 (Figure S1). In addition, this thermolabile mutant can form both mature (190 kDa) and immature protein (170 kDa) at 27°C,[35] detected with 897.2.[36] However, regardless of whether this mutant forms mature or immature protein, they cannot be detected with our MRP1/ABCC1 mAb 42.4 (Figure S1) mainly because F728 is part of this mAb's epitope.[36] In other words, once this deletion is corrected, the corrected version can be detected with either 897.2 or 42.4. Thus, our mAbs and ΔF728 mutated MRP1/ABCC1 provide an excellent model system for optimization of genome editing with the CRISPR/Cas9 system.

Effects of gRNAs Complementary to MRP1/ABCC1-ΔF728 Deletion Mutant on Knock In of the Three Deleted Nucleotides

The first set of gRNA was designed to cover the MRP1/ABCC1-ΔF728 deletion region, but artificially inserted a G at the beginning of the shorter gRNA1 (Figure 1A; Table 1). The second set of gRNA was designed to cover the MRP1/ABCC1-ΔF728 deletion region with a longer version of gRNA2 without any modification (Figure 1A; Table 1). These two sets of gRNAs were cloned into either pSpCas9(BB)-2A-GFP or pSpCas9n(BB)-2A-GFP (Table 1) and used to transfect MRP1/ABCC1-ΔF728-expressing baby hamster kidney (BHK) cells (Table 2, groups 1–12). The results in Figure 1B and Table 2 indicated that the gRNA alone (Table 2, groups 1, 4, 7, and 10), regardless of whether these gRNAs are the shorter or longer version and regardless of whether they were cloned in Cas9 or Cas9n vector, or donor DNA along with GFP-expressing Cas9 or Cas9n

Table 1. gRNA Constructs

Name	Vector	Sequence
Cas9.gRNA1	pSpCas9(BB)-2A-GFP	5′-GAAACATCCTT—GGATGTCAGC-3′
Cas9n.gRNA1	pSpCas9n(BB)-2A-GFP	5′-GAAACATCCTT—GGATGTCAGC-3′
Cas9.gRNA2	pSpCas9(BB)-2A-GFP	5′-GAAAACATCCTT—GGATGTCAG CTGG-3′
Cas9n.gRNA2	pSpCas9n(BB)-2A-GFP	5′-GAAAACATCCTT—GGATGTCAG CTGG-3′
Cas9.gRNA3	pSpCas9(BB)-2A-GFP	5′-GCATCCTTTTTGGATGTCAGC-3′
Cas9n.gRNA3	pSpCas9n(BB)-2A-GFP	5′-GCATCCTTTTTGGATGTCAGC-3′
Cas9.gRNA4	pSpCas9(BB)-2A-GFP	5′-GAAAACATCCTTTTTGGATGTCA GCTGG-3′
Cas9n.gRNA4	pSpCas9n(BB)-2A-GFP	5′-GAAAACATCCTTTTTGGATGTCA GCTGG-3′
Cas9.gRNA5	pSpCas9(BB)-2A-GFP	5′-GCCTATGTGCCACAGCAGGCC-3′
Cas9.gRNA6	pSpCas9(BB)-2A-GFP	5′-TGATACAGGCCTGTGCCCCTC-3′

vectors (Figure 1B; Table 2, groups 3, 6, 9, and 12), did not yield a protein detected by 42.4 mAb, indicating that gRNA alone or donor DNA plus GFP-expressing Cas9 or Cas9n vector cannot efficiently induce the HDR reaction between the WT donor DNA and the MRP1/ABCC1-ΔF728 target. In contrast, co-transfection of the shorter version, Cas9.gRNA1, with WT donor DNA yielded a clear band at the position of mature MRP1/ABCC1 (Figure 1B, group 2), whereas co-transfection of the longer version, i.e., Cas9.gRNA2, with WT donor DNA did not yield a detectable amount of mature MRP1/ABCC1 (Figure 1B; Table 2, group 8), suggesting that the longer version of Cas9.gRNA2 may not fit for Cas9's function. In addition, co-transfection of Cas9n.gRNA1 or Cas9n.gRNA2 with WT donor DNA also did not yield a detectable amount of mature MRP1/ABCC1 (Figure 1B; Table 2, groups 5 and 11), suggesting that a Cas9n-mediated nick may not be sufficient to efficiently induce the HDR reaction between the MRP1/ABCC1-ΔF728 deletion target DNA and the WT donor DNA.

The individual colonies isolated from group 2 were screened with MRP1/ABCC1 mAb 42.4 (Figure 1C), and 29.2% of the colonies were positive (Table 2, group 2). In order to further confirm that the three deleted nucleotides were knocked in by this treatment, we used total RNA isolated from colony 2-12 (Figure 1C) to do reverse transcription, PCR amplification, and cloning. Sequence analysis of 23 clones showed that 2 of them had perfect insertion of the deleted 3 nt in ΔF728 (type 1 in Figure 1D); 3 of them had perfect sequence from the host, i.e., BHK cell (type 2 in Figure 1D); 12 of them had deletion mutations (types 3, 4, 5, and 9 in Figure 1D); 3 of them had a one nucleotide insertion (types 6 and 7 in Figure 1D); and 3 of them had deleted 16 nt and inserted 75 nt in the deleted region (type 8 in Figure 1D), reflecting the domination of HDR by NHEJ of the modified DNA ends.

Effects of gRNAs Complementary to WT MRP1/ABCC1 on Knock In of the Three Deleted Nucleotides

The results described above indicated that the NHEJ of the ends generated by Cas9.gRNA1 that perfectly matched with the ΔF728 deletion target dominates the HDR to correct the three-nucleotide deletion, suggesting that this kind of gRNA is not ideal for gene correction. Therefore, new sets of gRNAs were designed (Table 1; Figure 2A). The first set of gRNA was designed to cover the F728 region, but artificially inserted a G at the beginning of the shorter gRNA (Figure 2A, gRNA3; Table 1, Cas9.gRNA3 and Cas9n.gRNA3). The second set of gRNA was designed to cover the F728 region with longer version without any artificial modification (Figure 2A, gRNA4; Table 1, Cas9.gRNA4 and Cas9n.gRNA4). Upon transfection of MRP1/ABCC1-ΔF728-expressing BHK cells with these gRNAs, whole cell lysates were analyzed by western blot probed with mAb 42.4. The results in Figure 2B and Table 2 indicated that gRNA alone (Figure 2B and Table 2, groups 13, 16, 19, and 22) or donor DNA plus Cas9 vector (Figure 2B and Table 2, groups 15, 18, 21, and 24) did not yield a protein detected by mAb 42.4, suggesting that gRNA alone or donor DNA along with vector cannot efficiently induce the HDR reaction between the WT donor DNA and the ΔF728 mutated target. In contrast, co-transfection of Cas9.gRNA3 with WT donor DNA yielded a clear band at the position of mature MRP1/ABCC1 (Figure 2B and Table 2, group 14), whereas co-transfection of Cas9n.gRNA3 (Table 2, group 17) with WT donor DNA did not yield a detectable amount of mature MRP1 (Figure 2B, group 17), suggesting that the nicks made by Cas9n do not efficiently induce the HDR reaction between the WT donor DNA and the ΔF728 deletion target. In addition, co-transfection of the longer version Cas9.gRNA4 or Cas9n.gRNA4 with WT donor DNA (Table 2, groups 20 and 23) also did not yield a detectable amount of mature MRP1 (Figure 2B, groups 20 and 23), suggesting that the shorter version of the gRNA fits with the Cas9, whereas the longer version does not efficiently fit the Cas9 enzyme.

The individual colonies isolated from group 14 were screened with MRP1/ABCC1 mAb 42.4 (Figure 2C), and 6.5% of the colonies screened were positive (Table 2, group 14). These results were further verified by using mAb 897.2 to detect both the mature form, i.e., the corrected form, and the immature form, i.e., the original ΔF728 (Figure S2). In order to further confirm the three deleted nucleotides were knocked in by this treatment, we used total RNA isolated from colony 14-41 (Figure 2C) to do reverse transcription, PCR amplification, and cloning. Sequence analyses of 107 clones showed that 4 of them had perfect insertion of the deleted 3 nt in ΔF728 (type 2 in Figure 2D) and 103 of them had perfect ΔF728 sequence (type 1 in Figure 2D). Interestingly, we have not found any mutation in the amplified fragment (from 2,224 to 2,590) covering the F728 region, suggesting that the Cas9.gRNA3-mediated cutting mainly occurred at the WT donor DNA. These results also suggested that the rate of HDR induced by Cas9.gRNA3 is low, but this treatment significantly reduced the possibility of introducing new mutations into our interested target gene.

Table 2. The Effects of Variant gRNAs on Homology-Directed Recombination

Transfection Group No.	Cas and gRNA	Donor	WT MRP1 in Mixed Population	Total Colonies Analyzed	MRP1- Positive Colonies
1	Cas9.gRNA1	N/A	N/A	N/A	
2	Cas9.gRNA1	WT donor	Yes	24	7
3	Cas9	WT donor	N/A	N/A	
4	Cas9n.gRNA1	N/A	N/A	N/A	
5	Cas9n.gRNA1	WT donor	N/A	N/A	
6	Cas9n	WT donor	N/A	N/A	
7	Cas9.gRNA2	N/A	N/A	N/A	
8	Cas9.gRNA2	WT donor	N/A	N/A	
9	Cas9	WT donor	N/A	N/A	
10	Cas9n.gRNA2	N/A	N/A	N/A	
11	Cas9n.gRNA2	WT donor	N/A	N/A	
12	Cas9n	WT donor	N/A	N/A	
13	Cas9.gRNA3	N/A	N/A	N/A	
14	Cas9.gRNA3	WT donor	Yes	46	3
15	Cas9	WT donor	N/A	N/A	
16	Cas9n.gRNA3	N/A	N/A	N/A	
17	Cas9n.gRNA3	WT donor	N/A	N/A	
18	Cas9n	WT donor	N/A	N/A	
19	Cas9.gRNA4	N/A	N/A	N/A	
20	Cas9.gRNA4	WT donor	N/A	N/A	
21	Cas9	WT donor	N/A	N/A	
22	Cas9n.gRNA4	N/A	N/A	N/A	
23	Cas9n.gRNA4	WT donor	N/A	N/A	
24	Cas9n	WT donor	N/A	N/A	
25	Cas9.gRNA5	N/A	N/A	N/A	
26	Cas9.gRNA5	WT donor	N/A	N/A	
27	Cas9.gRNA5	5′ mut donor	N/A	N/A	
28	Cas9	WT donor + 5′ mut donor	N/A	N/A	
29	Cas9.gRNA6	N/A	N/A	N/A	
30	Cas9.gRNA6	WT donor	N/A	N/A	
31	Cas9.gRNA6	3′ mut donor	N/A	N/A	
32	Cas9	WT donor + 3′ mut donor	N/A	N/A	
33	Cas9.gRNA1+Cas9.gRNA3	WT donor	Yes	24	1
34	Cas9.gRNA1+Cas9.gRNA5	WT donor	N/A	N/A	
35	Cas9.gRNA1+Cas9.gRNA6	WT donor	N/A	N/A	

mut, mutation.

Effects of gRNAs Complementary to the 5′ Side or 3′ Side of the MRP1/ABCC1-ΔF728 Deletion Target Site on Knock In of the Three Deleted Nucleotides

The results in the previous section indicated that Cas9.gRNA3 complementary to WT donor DNA resulted in extremely low frequency of mutation in the region of interest. In this section, we test the effects of gRNAs complementary to both target DNA and WT donor DNA on knocking in of the three deleted nucleotides. We have designed gRNA5, 36 bp upstream of the ΔF728 deletion mutant, and gRNA6, 34 bp downstream of the ΔF728 target site (Figure 3A). In the meantime, we have generated mutated donor DNAs so that gRNA5 or gRNA6 will only recognize the target DNA, but not the donor DNA (Figure 3A). Upon transfection of MRP1/ABCC1-ΔF728-expressing BHK cells with these gRNAs, whole cell lysates were analyzed by western blot probed with mAb 42.4. The results in Figure 3B and Table 2 indicated that gRNA alone (Table 2, groups 25 and 29) or donor DNA

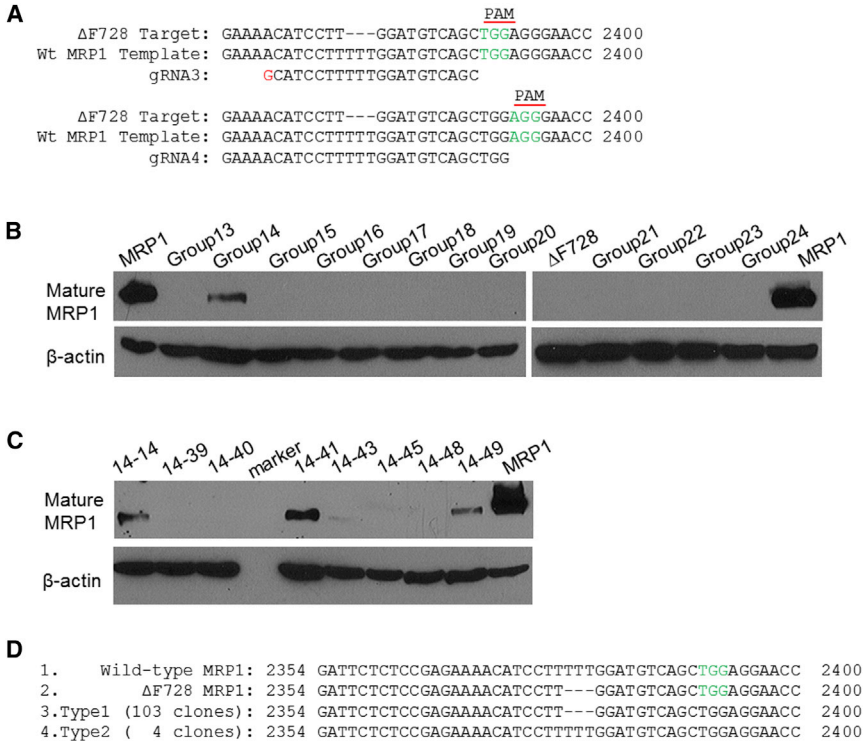

Figure 2. Effects of gRNAs Complementary to WT MRP1/ABCC1 on Knock In of the Three Deleted Nucleotides

(A) Design of gRNAs complementary to WT MRP1/ABCC1 donor DNA. The red G indicates an artificially introduced G residue at the beginning of the gRNA3. The minus sign (–) indicates the deleted nucleotide. The green TGG or AGG indicate the PAM sequence for gRNA3 or gRNA4. (B) A representative western blot, probed with MRP1/ABCC1 mAb 42.4, showing the WT MRP1/ABCC1 protein generated by HDR. (C) A representative western blot, probed with MRP1/ABCC1 mAb 42.4, showing the WT MRP1/ABCC1 protein generated by HDR in isolated individual colonies from transfection group 14. (D) DNA sequence analyses of the clones derived from the reverse transcription products of total RNA isolated from 14-41.

plus Cas9 vector (Table 2, groups 28 and 32) did not yield an amount of mature MRP1/ABCC1 protein detectable by mAb 42.4, suggesting that gRNA alone or donor DNA along with vector cannot efficiently induce the HDR reaction between the donor DNA and the ΔF728 mutated target DNA. In addition, co-transfection of Cas9.gRNA5 with WT donor DNA (Figure 3B and Table 2, group 26) or with mutated donor DNA (Figure 3B and Table 2, group 27) did not yield an amount of mature MRP1/ABCC1 protein detectable by mAb 42.4, suggesting that gRNA5 along with WT donor DNA or along with mutated donor DNA cannot efficiently induce the HDR reaction between the donor DNA and the ΔF728 mutated target DNA. Furthermore, co-transfection of Cas9.gRNA6 with WT donor DNA (Figure 3B and Table 2, group 30) or with mutated donor DNA (Figure 3B and Table 2, group 31) did not yield an amount of mature MRP1/ABCC1 protein detectable by mAb 42.4, suggesting that gRNA6 along with WT donor DNA or along with mutated donor DNA cannot efficiently induce the HDR reaction between the donor DNA and the ΔF728 mutated target DNA.

Because none of these treatments yielded an amount of mature MRP1/ABCC1 protein detectable by mAb 42.4, individual colonies were not isolated from these GFP-positive cells. In order to test whether these treatments generate mutations or correction of the ΔF728 deletion, we used total RNA isolated from mixtures of groups of 26, 27, 30, or 31 to do reverse transcription, PCR amplification, and cloning. Sequence analyses of 54 clones from group 26 showed that 49 of them had perfect ΔF728 sequence (type 1 in Figure 3C), 3 of them had a 10 nt deletion at the cutting site (type 2 in Figure 3C), 1 of them had a 1 nt deletion at the cutting site (type 4 in Figure 3C), and 1 of them had a 94-nt deletion (type 3 in Figure 3C), suggesting that cutting at the 5′ side of ΔF728 caused mutations. Sequence analyses of 50 clones from group 27 (type 5 in Figure 3C) or 56 clones from group 30 (type 1 in Figure 3D) showed no gene correction and no mutation. However, sequence analyses of 44 clones from group 31 showed that 40 of them had perfect ΔF728 sequence (type 2 in Figure 3D); 1 of them had perfect insertion of the deleted 3 nt in ΔF728 (type 3 in Figure 3D); 2 of them had perfect sequence from the host, i.e., BHK cell (type 4 in Figure 3D); and 1 of them had a single mutation at the 5′ side of ΔF728 (type 5 in Figure 3D), suggesting that cutting at the 3′ side of ΔF728 in target DNA caused gene correction and gene mutations.

Effects of Combination of gRNA1 with gRNA3, gRNA5, or gRNA6 on Knocking in of the Three Deleted Nucleotides

The findings described above indicated that gRNA5 or gRNA6 recognizing both target DNA and donor DNA at the 5′ side or 3′ side of the ΔF728 deletion mutant did not efficiently induce HDR between the ΔF728 mutated target DNA and the WT donor DNA. In contrast, gRNA1 recognizing the ΔF728 mutated target DNA or gRNA3 recognizing the WT donor DNA covering F728 did induce the HDR reaction between the ΔF728 mutated target DNA and the WT donor DNA. In this section, we test the effects of the combination of gRNA1 with gRNA3, gRNA5, or gRNA6 (Table 2) on knocking in of the three deleted nucleotides. The treatment with combination of gRNA1 and gRNA3 yielded a band at the position of mature MRP1/ABCC1 (Figure 4A), whereas the combination of gRNA1 with gRNA5 or gRNA6 did not yield any detectable amount of mature MRP1/ABCC1 (Figure 4A), suggesting that the rate of HDR induced by gRNA1 and gRNA3 is significantly higher than the combination of gRNA1 with gRNA5 or gRNA6.

The individual colonies isolated from group 33 were screened with MRP1/ABCC1 mAb 42.4 (Figure 4B), and 4.2% of the colonies

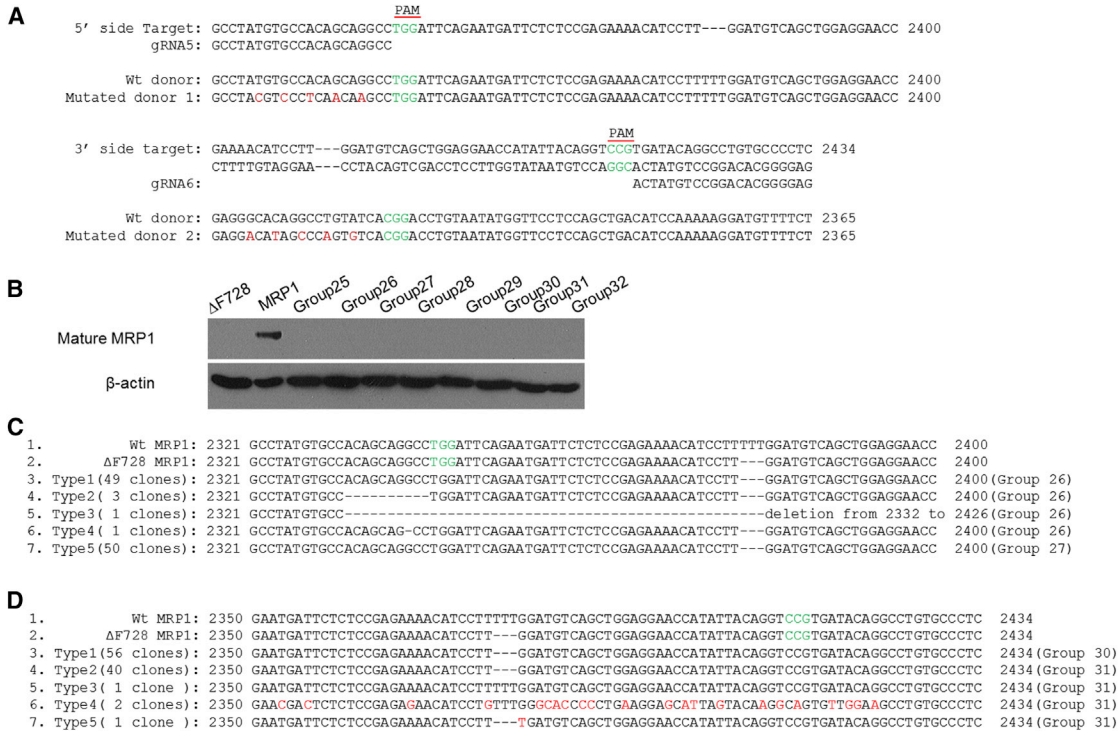

Figure 3. Effects of gRNAs Complementary to the 5′ Side or 3′ Side of the MRP1/ABCC1-ΔF728 Deletion Target Site on Knock In of the Three Deleted Nucleotides

(A) Design of donor DNA and gRNAs complementary to the 5′ side (gRNA5) or 3′ side (gRNA6) of the MRP1/ABCC1-ΔF728 deletion mutant. The minus sign (–) indicates the deleted nucleotide. The green TGG or CGG indicate the PAM sequence for gRNA5 or gRNA6. The sequences in WT donor indicate that gRNA5 or gRNA6 will not only recognize the target DNA sequence, but also the WT donor DNA sequence. The red capital letters in mutated donor 1 indicate that these nucleotides were mutated so that gRNA5 will not recognize the sequence in the mutated donor 1. The red capital letters in mutated donor 2 indicate that these nucleotides were mutated so that gRNA6 will not recognize the sequence in the mutated donor 2. (B) A representative western blot, probed with MRP1/ABCC1 mAb 42.4, showing that none of them has a detectable amount of WT MRP1/ABCC1 protein generated by HDR. (C) DNA sequence analyses of the clones derived from the reverse transcription products of total RNA isolated from group 26 or 27. (D) DNA sequence analyses of the clones derived from the reverse transcription products of total RNA isolated from group 30 or 31. The red capital letters indicate the sequences that are not complementary to human MRP1/ABCC1.

were positive (Table 2, group 33). In order to further confirm that the three deleted nucleotides were knocked in by this treatment, we used total RNA isolated from colony 33-10 (Figure 4B) to do reverse transcription, PCR amplification, and cloning. Sequence analyses of 91 clones showed that 12 of them had the original 3 nt deletion in ΔF728 (type 1 in Figure 4C), 11 had perfect insertion of the deleted 3 nt in ΔF728 (type 2 in Figure 4C), 50 had deletion mutations (types 3–9 in Figure 4C), 3 had 1 nt insertion (types 10 and 11 in Figure 4C), and 15 had 3 nt deletion and 9 nt insertion at the deletion site (type 12 in Figure 4C). Thus, although the treatment with gRNA1 and gRNA3 induced HDR reaction between the target DNA and the donor DNA, the NHEJ of the modified DNA ends dominates the HDR in a cloned cell line.

As shown in Figure 4, insertion of the 3 nt into the ΔF728 deletion site promoted the conversion of the immature ΔF728 variant into mature WT MRP1/ABCC1, suggesting that correction of the deletion restored its proper folding. To test whether the folded protein trafficked to the cell surface and restored its drug transport function, we assayed the ability of the cells to resist the cytotoxic action of daunorubicin. Indeed, the daunorubicin killing profile of MRP1/ABCC1-ΔF728-expressing cells is similar to BHK cells (Figure 4D), whereas the IC_{50} value of 33-10 is approximately 7.5-fold higher than that of BHK or MRP1/ABCC1-ΔF728-expressing cells (Figure 4E), suggesting that correction of these three-nucleotide deletions by CRISPR/Cas9-gRNA restored its drug transport function.

DISCUSSION

Development of the CRISPR/Cas9 system provides an opportunity to generate recombinogenic DNA ends near the mutation sites. However, the design of gRNAs is restricted by the available protospacer adjacent motif (PAM) and a guanine residue approximately 20 bp upstream of the PAM sequence near the mutation sites. We have found that our MRP1/ABCC1-ΔF728 deletion mutant, along with our MRP1/ABCC1 mAbs, provide an excellent model system to test the HDR-mediated repair of the three-nucleotide deletion mutation. We had found earlier that NHEJ efficiently occurred

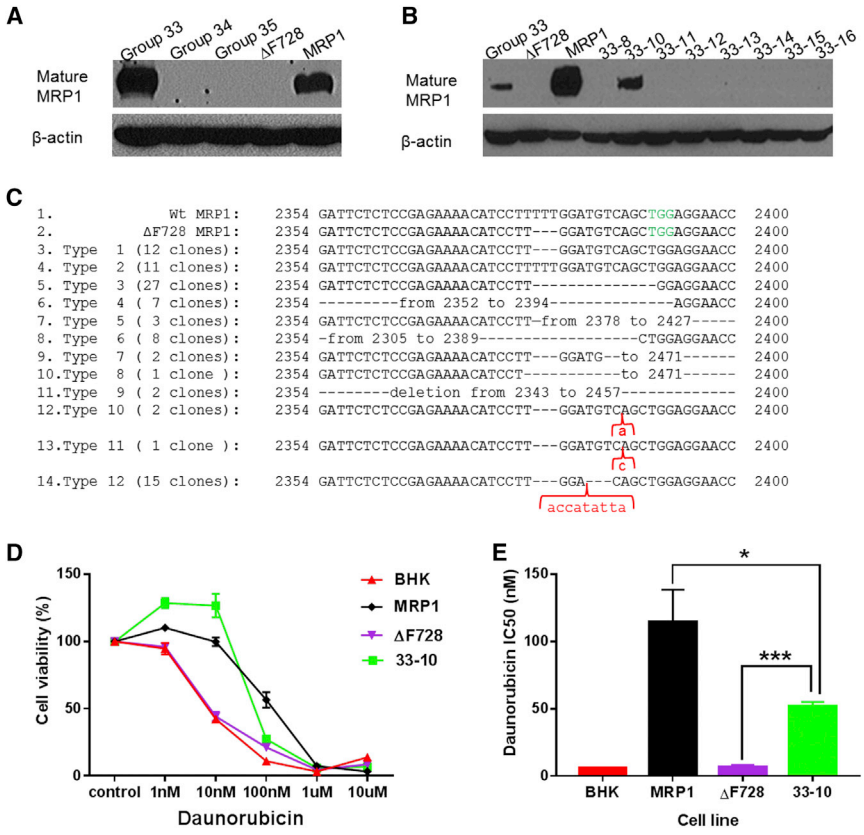

Figure 4. Effects of Combination of gRNA1 with gRNA3, gRNA5, or gRNA6 on Knock In of the Three Deleted Nucleotides

(A) A representative western blot, probed with MRP1/ABCC1 mAb 42.4, showing the WT MRP1/ABCC1 protein generated by HDR. (B) A representative western blot, probed with MRP1/ABCC1 mAb 42.4, showing the WT MRP1/ABCC1 protein generated by HDR in isolated individual colonies from transfection group 33. (C) DNA sequence analyses of the clones derived from the reverse transcription products of total RNA isolated from 33-10. The minus sign (–) indicates the deleted nucleotide. The small red letters indicate the inserted nucleotides. (D) Chemosensitivity assay of the BHK cells expressing the WT MRP1, ΔF728, and a recombinant clone (33-10) expressing WT MRP1 protein generated by CRISPR/Cas9 mediated HDR. (E) IC_{50} values (nM) of daunorubicin are: 6.03 ± 0.56 (BHK), 6.95 ± 1.38 (ΔF728), 114.45 ± 23.99 (MRP1), and 51.82 ± 3.37 (33-10). *p = 0.011; ***p < 0.0001.

for any DSB repair in mammalian cells.[30] In addition, we also had found that the modifications at the break sites[33] could cause deleterious mutations. Using our model system, we attempt to clarify the following three important issues: (1) whether gRNAs can be designed to increase the efficiency of the HDR-mediated repair of the three-nucleotide deletion mutation, (2) whether gRNAs can be designed to increase the safety of the CRISPR/Cas9-gRNA mediated HDR, and (3) whether the CRISPR/Cas9.gRNA-donor DNA system can be designed to create a PAM sequence near the site of interest.

The result presented in Table 2 indicated that the rate of HDR mediated by gRNA complementary to target DNA (Table 2, group 2) is approximately 29%, which is comparable with the experiments done in other cell systems.[37–39] This rate is significantly higher than that using gRNAs complementary to the donor DNA (Figure S3; Table 2, group 2 versus group 14), suggesting that the efficiency of HDR mediated by the DSB in target DNA is significantly higher than the DSB in donor DNA. We further investigated whether the combination of these gRNAs would have a significant effect on HDR. It turned out that the rate of HDR induced by these two gRNAs (Table 2, group 33) is slightly less than with gRNA complementary to donor DNA alone (Figure S3; Table 2, group 33 versus group 14). Interestingly, regardless of whether the DSB was induced by gRNA complementary to target DNA (Table2, group 2) or to donor DNA (Table 2, group 14), the rate of HDR induced by DSB is significantly higher than when the nick is at the same location generated by Cas9n (Table 2, group 2 versus group 5 or group 14 versus group 17), suggesting that nicks generated by Cas9n do not efficiently induce HDR. Further investigation indicated that the rates of HDR induced by gRNA located 36 bp upstream or 34 bp downstream of the deletion mutant ΔF728 are significantly lower than the gRNAs closer to the deletion mutation (Table 2, group 2 versus group 27, group 2 versus group 31, group 33 versus group 26, group 33 versus group 30), suggesting that the rate of HDR induced by DSB is directly associated with the distance of mutation from the DSB site. This conclusion is consistent with that of another study.[40] However, it has also been recently reported that gRNA located 87 bp upstream of the deletion mutant CFTR-ΔF508 induced HDR.[41] Our sequence analysis also confirmed that the gRNA located 34 bp downstream of the deletion mutant ΔF728 induced HDR (Figure 3D, type 3).

The correction of three nucleotide deletion in CFTR-ΔF508 has been achieved in either induced pluripotent stem cells[42–44] or cystic fibrosis patient-derived organoids.[38] However, modification of the ends generated by DSB and the NHEJ-mediated mutation is still a big issue for genome editing.[41] Our sequencing data strongly support this conclusion. For example, the ratio of the precise knock in of the three deleted nucleotide and mutations, including deletion and insertion, that resulted from NHEJ is 1:10.5 if the gRNA complementary to the target DNA is used (Figure 1D), and this ratio is slightly lower (1:6.2) when gRNAs complementary to target DNA and donor DNA are used (Figure 4C). In contrast, only precisely modified product was found when gRNA complementary to WT donor DNA was used (Figure 2D), meaning that this gRNA

Table 3. List of Oligonucleotides

Number	Name	Sequence
1	gRNA1-forward	5′-CACCGAAACATCCTTGGATGTCAGC-3′
2	gRNA1-reverse	5′-AAACGCTGACATCCAAGGATGTTTC-3′
3	gRNA2-forward	5′-CACCGAAAACATCCTTGGATGTCAG CTGG-3′
4	gRNA2-reverse	5′-AAACCCAGCTGACATCCAAGGATGT TTTC-3′
5	gRNA3-forward	5′-CACCGCATCCTTTTTGGATGTCAGC-3′
6	gRNA3-reverse	5′-AAACGCTGACATCCAAAAAGGATGC-3′
7	gRNA4-forward	5′-CACCGAAAACATCCTTTTTGGATGT CAGCTGG-3′
8	gRNA4-reverse	5′-AAACCCAGCTGACATCCAAAAAGGAT GTTTTC-3′
9	gRNA5-forward	5′-CACCGCCTATGTGCCACAGCAGGCC-3′
10	gRNA5-reverse	5′-AAACGGCCTGCTGTGGCACATAGGC-3′
11	gRNA6-forward	5′-CACCGAGGGCACAGGCCTGTATCA-3′
12	gRNA6-reverse	5′-AAACTGATACAGGCCTGTGCCCTC-3′
13	gRNA5-mut-forward	5′-CAAGGGCTCCGTGGCCTACGTCCCT CAACAAGCCTGGATTCAGAATG-3′
14	gRNA5-mut-reverse	5′-CATTCTGAATCCAGGCTTGTTGAGG GACGTAGGCCACGGAGCCCTTG-3′
15	gRNA6-mut-forward	5′-CATATTACAGGTCCGTGACACTGGG CTATGTCCTCCTCCCAGACCTGG-3′
16	gRNA6-mut-reverse	5′-CCAGGTCTGGGAGGAGGACATAGC CCAGTGTCACGGACCTGTAATATG-3′
17	MRP1.C682A-forward	5′-GGTGGGCCAGGTGGGCGCCGGAAA GTTGTCCCTGC-3′
18	MRP1.D792A-reverse	5′-CACTGCTGAGAGGGGATCAGCGAA GAGGTAAATGTC-3′
19	MRP1-6A	5′-TACACGGAAAGCTTGACCTGCCCT-3′
20	T3 primer	5′-AATTAACCCTCACTAAAGGG-3′

preferentially binds to the donor DNA and makes a DSB at the donor DNA. This result was also interpreted as that the mutations introduced by the DSB occurred at the donor DNA, but not at the target DNA. Off-target site searching from human genome for this gRNA3 revealed that there is only one nucleotide sequence (5′-CATCCTTTcTGGATtTCAGaTGG-3′) located on human chromosome 3 that has three mismatches with this gRNA (with 575 score considering the score of gRNA as 1,000). Previous studies indicated that off-target effects are limited to sites with only one to three mismatches,[28] suggesting that gRNA3 complementary to donor DNA should have minimum off-target effects. This result provides a great opportunity for us to design gRNAs based on the following modifications in the donor DNA: (1) to make silent mutations to create a PAM sequence near the target site, (2) to make silent mutations to introduce a guanine residue approximately 20 bp upstream of the PAM sequence, and (3) to make silent mutations so that the gRNA will have minimum off-target effects. In this case, the gRNAs will preferentially recognize the modified donor DNA and make a DSB at the modified donor DNA. Thus, the data presented here provide important guidelines for gRNA and donor DNA design for genome editing.

MATERIALS AND METHODS

Materials

Most of the chemicals, including daunorubicin and 3-[4,5-dimethylthiazol-2-yl]-2,5-diphenyl-tetrazolium bromide (MTT), were purchased from Sigma. DMEM/F-12 medium and fetal bovine serum were derived from Thermo Scientific. QuikChange site-directed mutagenesis kit was from Stratagene. Anti-mouse Ig conjugated with horseradish peroxidase was from Amersham Biosciences. Chemiluminescent substrates for western blotting were from Pierce. pSpCas9(BB)-2A-GFP (PX458) and pSpCas9n(BB)-2A-GFP (PX461) were derived from Addgene.

Cell Lines, Cell Culture, and Transfection

WT MRP1/ABCC1[45] and MRP1/ABCC1-ΔF728-expressing BHK cells[35] were grown in DMEM/F-12 medium containing 5% fetal bovine serum at 37°C in 5% CO_2. Subconfluent cells were transfected with plasmid DNAs listed in Table 1 in the presence of 20 mM 4-(2-hydroxyethyl)-1-piperazineethanesulfonic acid (HEPES; pH 7.05), 137 mM NaCl, 5 mM KCl, 0.7 mM Na_2HPO_4, 6 mM dextrose, and 125 mM $CaCl_2$.[45] GFP-positive cells, 14 days post-transfection, were sorted out in our Flow Cytometry Core with BD FACSDiva software. Individual colonies were picked and analyzed once the WT MRP1/ABCC1 protein was detected with 42.4 mAb from a whole mixture of GFP-positive cell lysates.

gRNAs and Donor Plasmid Construction

The annealed gRNAs (Table 3), such as gRNA1-forward and gRNA1-reverse, were cloned into the BbsI digested pSpCas9(BB)-2A-GFP or pSpCas9n(BB)-2A-GFP (Table 1), and the inserted gRNAs were confirmed by DNA sequencing. The WT donor DNA was generated by insertion of the BamHI (1036)-EcoRI (4076) MRP1/ABCC1 cDNA fragment into pBluescript (named as pB.MRP1.WT-donor5). In order to generate mutated donor DNAs so that gRNA5 or gRNA6 will not efficiently bind to them, we mutated the five residues within the gRNA5 or gRNA6 (Figure 3A) region in pB.MRP1.WT-donor5 (without changing amino acid sequences) by using the corresponding forward/reverse primers listed in Table 3 and the QuikChange site-directed mutagenesis kit from Stratagene.[36] Regions containing these mutations were sequenced to confirm that the correct clones were obtained.

RNA Extraction, Reverse Transcription, PCR Amplification, Cloning, and Sequence Analysis

Total RNA was isolated from BHK cells with RNeasy Mini kit from QIAGEN, according to the protocol provided by the manufacturer. Reverse transcription, with MRP1-6A (Table 3) as primer, was performed with RT first strand kit from QIAGEN, according to the protocol provided by QIAGEN. The reverse transcription products were used as a template to amplify the 367 bp (from 2,224 to 2,590) fragment with MRP1.C682A-forward and MRP1.D792A-reverse primers (Table 3). The amplified fragments were cloned into pBluescript and sequenced with T3 primer (Table 3).

Identification of the MRP1/ABCC1 Protein

Western blot was performed according to the method described previously.[36] 42.4 mAb was used to identify the WT MRP1/ABCC1 protein, whereas 897.2 mAb was used to detect the WT MRP1/ABCC1 protein and the MRP1/ABCC1-ΔF728 mutated protein. The secondary antibody used was anti-mouse Ig conjugated with horseradish peroxidase. Chemiluminescent film detection was performed according to the manufacturer's recommendations (Pierce).

Chemosensitivity Assay

The daunorubicin sensitivities of BHK cells expressing variant MRP1/ABCC1 proteins were determined by employing the CCK-8 cytotoxicity assay. In brief, cells were plated in a volume of 90 μL at 3,000 cells per well in 96-well plates. After incubation at 37°C overnight, 10 μL of the media containing varying concentrations of daunorubicin was added to the wells and incubated for an additional 4 days at 37°C. At the end of drug exposure, 10 μL of CCK-8 solution was added to each well and incubated for 1–4 hr. The absorbance at 450 nm was determined by using Universal Microplate Spectrophotometer derived from BioTek.

Statistical Analysis

The results in Figure 4E were presented as means ± SD from the triplicate experiments. The two-tailed p values were calculated based on the unpaired t test from GraphPad Software Quick Calcs. By conventional criteria, if $p < 0.05$, the difference between two samples is considered to be statistically significant.

SUPPLEMENTAL INFORMATION

Supplemental Information includes three figures and can be found with this article online at http://dx.doi.org/10.1016/j.omtn.2017.05.005.

AUTHOR CONTRIBUTIONS

X.C. contributed to conception and design of the study. Q.X., Y.H., and X.C. contributed to acquisition of the data. X.C. and Q.X. wrote the manuscript. All of the authors contributed to interpretation of the data and provided input for the manuscript.

CONFLICTS OF INTEREST

The authors declare no competing financial interests.

ACKNOWLEDGMENTS

The authors would like to thank Leah W. Moore for participating in manuscript preparation.

REFERENCES

1. Nathans, J., Davenport, C.M., Maumenee, I.H., Lewis, R.A., Hejtmancik, J.F., Litt, M., Lovrien, E., Weleber, R., Bachynski, B., Zwas, F., et al. (1989). Molecular genetics of human blue cone monochromacy. Science *245*, 831–838.

2. Weitz, C.J., Miyake, Y., Shinzato, K., Montag, E., Zrenner, E., Went, L.N., and Nathans, J. (1992). Human tritanopia associated with two amino acid substitutions in the blue-sensitive opsin. Am. J. Hum. Genet. *50*, 498–507.

3. Winderickx, J., Sanocki, E., Lindsey, D.T., Teller, D.Y., Motulsky, A.G., and Deeb, S.S. (1992). Defective colour vision associated with a missense mutation in the human green visual pigment gene. Nat. Genet. *1*, 251–256.

4. Mackey, D.A. (1994). Three subgroups of patients from the United Kingdom with Leber hereditary optic neuropathy. Eye (Lond.) *8*, 431–436.

5. Kerem, B., Rommens, J.M., Buchanan, J.A., Markiewicz, D., Cox, T.K., Chakravarti, A., Buchwald, M., and Tsui, L.C. (1989). Identification of the cystic fibrosis gene: genetic analysis. Science *245*, 1073–1080.

6. Bobadilla, J.L., Macek, M., Jr., Fine, J.P., and Farrell, P.M. (2002). Cystic fibrosis: a worldwide analysis of CFTR mutations–correlation with incidence data and application to screening. Hum. Mutat. *19*, 575–606.

7. Feder, J.N., Gnirke, A., Thomas, W., Tsuchihashi, Z., Ruddy, D.A., Basava, A., Dormishian, F., Domingo, R., Jr., Ellis, M.C., Fullan, A., et al. (1996). A novel MHC class I-like gene is mutated in patients with hereditary haemochromatosis. Nat. Genet. *13*, 399–408.

8. Pietrangelo, A., Montosi, G., Totaro, A., Garuti, C., Conte, D., Cassanelli, S., Fraquelli, M., Sardini, C., Vasta, F., and Gasparini, P. (1999). Hereditary hemochromatosis in adults without pathogenic mutations in the hemochromatosis gene. N. Engl. J. Med. *341*, 725–732.

9. Gitschier, J., Wood, W.I., Tuddenham, E.G., Shuman, M.A., Goralka, T.M., Chen, E.Y., and Lawn, R.M. (1985). Detection and sequence of mutations in the factor VIII gene of haemophiliacs. Nature *315*, 427–430.

10. Rees, D.J., Rizza, C.R., and Brownlee, G.G. (1985). Haemophilia B caused by a point mutation in a donor splice junction of the human factor IX gene. Nature *316*, 643–645.

11. Bentley, A.K., Rees, D.J., Rizza, C., and Brownlee, G.G. (1986). Defective propeptide processing of blood clotting factor IX caused by mutation of arginine to glutamine at position -4. Cell *45*, 343–348.

12. Davis, L.M., McGraw, R.A., Ware, J.L., Roberts, H.R., and Stafford, D.W. (1987). Factor IXAlabama: a point mutation in a clotting protein results in hemophilia B. Blood *69*, 140–143.

13. Youssoufian, H., Kazazian, H.H., Jr., Phillips, D.G., Aronis, S., Tsiftis, G., Brown, V.A., and Antonarakis, S.E. (1986). Recurrent mutations in haemophilia A give evidence for CpG mutation hotspots. Nature *324*, 380–382.

14. Diuguid, D.L., Rabiet, M.J., Furie, B.C., Liebman, H.A., and Furie, B. (1986). Molecular basis of hemophilia B: a defective enzyme due to an unprocessed propeptide is caused by a point mutation in the factor IX precursor. Proc. Natl. Acad. Sci. USA *83*, 5803–5807.

15. Gitschier, J., Wood, W.I., Shuman, M.A., and Lawn, R.M. (1986). Identification of a missense mutation in the factor VIII gene of a mild hemophiliac. Science *232*, 1415–1416.

16. DiLella, A.G., Marvit, J., Brayton, K., and Woo, S.L. (1987). An amino-acid substitution involved in phenylketonuria is in linkage disequilibrium with DNA haplotype 2. Nature *327*, 333–336.

17. Lyonnet, S., Caillaud, C., Rey, F., Berthelon, M., Frézal, J., Rey, J., and Munnich, A. (1989). Molecular genetics of phenylketonuria in Mediterranean countries: a mutation associated with partial phenylalanine hydroxylase deficiency. Am. J. Hum. Genet. *44*, 511–517.

18. Bisceglia, M., Galliani, C.A., Senger, C., Stallone, C., and Sessa, A. (2006). Renal cystic diseases: a review. Adv. Anat. Pathol. *13*, 26–56.

19. Audrézet, M.P., Cornec-Le Gall, E., Chen, J.M., Redon, S., Quéré, I., Creff, J., Bénech, C., Maestri, S., Le Meur, Y., and Férec, C. (2012). Autosomal dominant polycystic kidney disease: comprehensive mutation analysis of PKD1 and PKD2 in 700 unrelated patients. Hum. Mutat. *33*, 1239–1250.

20. Cheng, S.H., Gregory, R.J., Marshall, J., Paul, S., Souza, D.W., White, G.A., O'Riordan, C.R., and Smith, A.E. (1990). Defective intracellular transport and processing of CFTR is the molecular basis of most cystic fibrosis. Cell *63*, 827–834.

21. Denning, G.M., Anderson, M.P., Amara, J.F., Marshall, J., Smith, A.E., and Welsh, M.J. (1992). Processing of mutant cystic fibrosis transmembrane conductance regulator is temperature-sensitive. Nature *358*, 761–764.

22. Jinek, M., Chylinski, K., Fonfara, I., Hauer, M., Doudna, J.A., and Charpentier, E. (2012). A programmable dual-RNA-guided DNA endonuclease in adaptive bacterial immunity. Science *337*, 816–821.

23. Pennisi, E. (2013). The CRISPR craze. Science *341*, 833–836.

24. Ran, F.A., Hsu, P.D., Wright, J., Agarwala, V., Scott, D.A., and Zhang, F. (2013). Genome engineering using the CRISPR-Cas9 system. Nat. Protoc. *8*, 2281–2308.

25. Ran, F.A., Hsu, P.D., Lin, C.Y., Gootenberg, J.S., Konermann, S., Trevino, A.E., Scott, D.A., Inoue, A., Matoba, S., Zhang, Y., and Zhang, F. (2013). Double nicking by RNA-guided CRISPR Cas9 for enhanced genome editing specificity. Cell *154*, 1380–1389.

26. Cong, L., Ran, F.A., Cox, D., Lin, S., Barretto, R., Habib, N., Hsu, P.D., Wu, X., Jiang, W., Marraffini, L.A., and Zhang, F. (2013). Multiplex genome engineering using CRISPR/Cas systems. Science *339*, 819–823.

27. Fu, Y., Foden, J.A., Khayter, C., Maeder, M.L., Reyon, D., Joung, J.K., and Sander, J.D. (2013). High-frequency off-target mutagenesis induced by CRISPR-Cas nucleases in human cells. Nat. Biotechnol. *31*, 822–826.

28. Mali, P., Aach, J., Stranges, P.B., Esvelt, K.M., Moosburner, M., Kosuri, S., Yang, L., and Church, G.M. (2013). CAS9 transcriptional activators for target specificity screening and paired nickases for cooperative genome engineering. Nat. Biotechnol. *31*, 833–838.

29. Hsu, P.D., Scott, D.A., Weinstein, J.A., Ran, F.A., Konermann, S., Agarwala, V., Li, Y., Fine, E.J., Wu, X., Shalem, O., et al. (2013). DNA targeting specificity of RNA-guided Cas9 nucleases. Nat. Biotechnol. *31*, 827–832.

30. Chang, X.B., and Wilson, J.H. (1987). Modification of DNA ends can decrease end joining relative to homologous recombination in mammalian cells. Proc. Natl. Acad. Sci. USA *84*, 4959–4963.

31. Smithies, O., Gregg, R.G., Boggs, S.S., Koralewski, M.A., and Kucherlapati, R.S. (1985). Insertion of DNA sequences into the human chromosomal beta-globin locus by homologous recombination. Nature *317*, 230–234.

32. Thomas, K.R., Folger, K.R., and Capecchi, M.R. (1986). High frequency targeting of genes to specific sites in the mammalian genome. Cell *44*, 419–428.

33. Roth, D.B., Chang, X.B., and Wilson, J.H. (1989). Comparison of filler DNA at immune, nonimmune, and oncogenic rearrangements suggests multiple mechanisms of formation. Mol. Cell. Biol. *9*, 3049–3057.

34. Lieber, M.R. (2010). The mechanism of double-strand DNA break repair by the nonhomologous DNA end-joining pathway. Annu. Rev. Biochem. *79*, 181–211.

35. Gentzsch, M., Choudhury, A., Chang, X.B., Pagano, R.E., and Riordan, J.R. (2007). Misassembled mutant DeltaF508 CFTR in the distal secretory pathway alters cellular lipid trafficking. J. Cell Sci. *120*, 447–455.

36. Hou, Y., Cui, L., Riordan, J.R., and Chang, X. (2000). Allosteric interactions between the two non-equivalent nucleotide binding domains of multidrug resistance protein MRP1. J. Biol. Chem. *275*, 20280–20287.

37. Urnov, F.D., Miller, J.C., Lee, Y.L., Beausejour, C.M., Rock, J.M., Augustus, S., Jamieson, A.C., Porteus, M.H., Gregory, P.D., and Holmes, M.C. (2005). Highly efficient endogenous human gene correction using designed zinc-finger nucleases. Nature *435*, 646–651.

38. Schwank, G., Koo, B.K., Sasselli, V., Dekkers, J.F., Heo, I., Demircan, T., Sasaki, N., Boymans, S., Cuppen, E., van der Ent, C.K., et al. (2013). Functional repair of CFTR by CRISPR/Cas9 in intestinal stem cell organoids of cystic fibrosis patients. Cell Stem Cell *13*, 653–658.

39. Byrne, S.M., Ortiz, L., Mali, P., Aach, J., and Church, G.M. (2015). Multi-kilobase homozygous targeted gene replacement in human induced pluripotent stem cells. Nucleic Acids Res. *43*, e21.

40. Elliott, B., Richardson, C., Winderbaum, J., Nickoloff, J.A., and Jasin, M. (1998). Gene conversion tracts from double-strand break repair in mammalian cells. Mol. Cell. Biol. *18*, 93–101.

41. Hollywood, J.A., Lee, C.M., Scallan, M.F., and Harrison, P.T. (2016). Analysis of gene repair tracts from Cas9/gRNA double-stranded breaks in the human CFTR gene. Sci. Rep. *6*, 32230.

42. Firth, A.L., Menon, T., Parker, G.S., Qualls, S.J., Lewis, B.M., Ke, E., Dargitz, C.T., Wright, R., Khanna, A., Gage, F.H., and Verma, I.M. (2015). Functional gene correction for cystic fibrosis in lung epithelial cells generated from patient iPSCs. Cell Rep. *12*, 1385–1390.

43. Sargent, R.G., Suzuki, S., and Gruenert, D.C. (2014). Nuclease-mediated double-strand break (DSB) enhancement of small fragment homologous recombination (SFHR) gene modification in human-induced pluripotent stem cells (hiPSCs). Methods Mol. Biol. *1114*, 279–290.

44. Crane, A.M., Kramer, P., Bui, J.H., Chung, W.J., Li, X.S., Gonzalez-Garay, M.L., Hawkins, F., Liao, W., Mora, D., Choi, S., et al. (2015). Targeted correction and restored function of the CFTR gene in cystic fibrosis induced pluripotent stem cells. Stem Cell Reports *4*, 569–577.

45. Chang, X.B., Hou, Y.X., and Riordan, J.R. (1997). ATPase activity of purified multidrug resistance-associated protein. J. Biol. Chem. *272*, 30962–30968.